JACS
JOURNAL OF THE AMERICAN CHEMICAL SOCIETY

Communication

pubs.acs.org/JACS

Surface-Area-Dependent Electron Transfer Between Isoenergetic 2D Quantum Wells and a Molecular Acceptor

Benjamin T. Diroll,[†] Igor Fedin,[‡] Pierre Darancet,[†] Dmitri V. Talapin,[†,‡] and Richard D. Schaller*[,†,§]

[†]Center for Nanoscale Materials, Argonne National Laboratory, Lemont, Illinois 60439, United States

[‡]Department of Chemistry, University of Chicago, Chicago, Illinois 60637, United States

[§]Department of Chemistry, Northwestern University, Evanston, Illinois 60208, United States

Supporting Information

ABSTRACT: We report measurements of electron transfer rates for four isoenergetic donor−acceptor pairs comprising a molecular electron acceptor, methylviologen (MV), and morphology-controlled colloidal semiconductor nanoparticles of CdSe. The four nanoparticles include a spherical quantum dot (QD) and three differing lateral areas of 4-monolayer-thick nanoplatelets (NPLs), each with a 2.42 eV energy gap. As such, the measurements, performed via ultrafast photoluminescence, relate the dependence of charge transfer rate on the spatial extent of the initial electron−hole pair wave function explicitly, which we show for the first time to be related to surface area in this regime that is intermediate between homogeneous and heterogeneous charge transfer as well as 2D to 0D electron transfer. The observed nonlinear dependence of rate with surface area is attributed to exciton delocalization within each structure, which we show via temperature-dependent absorption measurements remains constant.

Controlled manipulations of charges into and out of nanosized particles are essential to the successful development of applications such as solution-processed solar cells, light-emitting diodes, lasers, and chem/bio sensors.[1,2] Several studies have investigated electron donor or acceptor species paired with spherical colloidal quantum dots (QDs) to evaluate rates and efficiencies of charge transfer (CT) in the context of Marcus Theory.[3−9] Frequent features of these studies include variation of CT driving force (free energy change) via either selection of different quencher molecules[10−12] or semiconductor energy-gap tuning via size-controlled quantum confinement.[5,13] Still other studies have characterized CT distance dependence via design of variable length spacers to separate quenchers or by ad-growth of shell spacer layers onto the redox-active QD core.[14−19] The number of quencher molecules in proximity to a nanoparticle directly impacts the observed CT rate owing to additive kinetics. As such, the bimolecular CT rate arising from the combination of one donor and one acceptor represents the constant of interest for comparison with modeling.[10,20−22]

The distance dependence of CT rates for weakly coupled organic chromophores in homogeneous solution generally follow exponential dependences.[23,24] For such molecular systems, redox center-to-center CT distance follows from examination of initial and final electron density or evaluation of the number of bonds between donor and acceptor for the well-defined case of intramolecular CT. CT involving QDs has mainly received consideration using this inner-sphere picture, but at the same time, donor−acceptor distance presents challenges to characterize and whether to implement the distance of a quencher to the QD particle center, or the distance from the particle surface remains unclear. Carrier delocalization over the entire quantum-confined particle intimates consideration of the former, whereas localized surface states or notions of enhanced electronic coupling at the interface bolster use of the latter. For nonspherical morphologies, this consideration becomes still more complex as a continuum of distances become relevant.

Here, we investigate bimolecular rates of CT between a well-known electron acceptor, methylviologen dichloride (MV), which might be considered as a zero-dimensional point in space, and an electron donor comprising either a spherical 2.4 nm diameter CdSe QD or one of several 2D CdSe nanoplatelets (NPLs) of controlled lateral dimension. In the presented series of measurements, the notion of center-to-center distance becomes especially challenging. Owing to fixed zinc-blende crystal structure, energy gap, and surface ligands of all examined nanoparticles, this study permits examination of such CT rate spatial dependence in 2D for the first time. The unique sample series permits us to examine the following questions. Will increasing lateral dimension for a fixed driving force yield a constant CT rate as Jablonski diagrams might relate, or how will the rate depend on particle spatial extent? We note that the presented experiments offer relevance to scenarios such as CT involving the broad range of emerging 2D semiconductor materials,[25] deleterious processes such as that of an individual defect in these systems that might produce carrier trapping over some distance, as well as insight into heterogeneous CT processes at interfaces more generally.

The development of colloidal NPLs affords precise synthetic control over the number of monolayers and concomitant narrow band-edge transition energy associated with the coherent motion of the exciton center of mass across the NPL.[26,27] Recently, it has become possible to control the lateral extent of fixed thickness NPL ensembles with nonzero, yet negligible changes in quantum confinement (see Figure 1 and Supporting Information).[28] At present, such control permits variation of surface area by a factor of ∼4 for a fixed thickness NPL ensemble (see Figure 1b). In

Received: June 26, 2016
Published: August 12, 2016

DOI: 10.1021/jacs.6b06572
J. Am. Chem. Soc. 2016, 138, 11109−11112

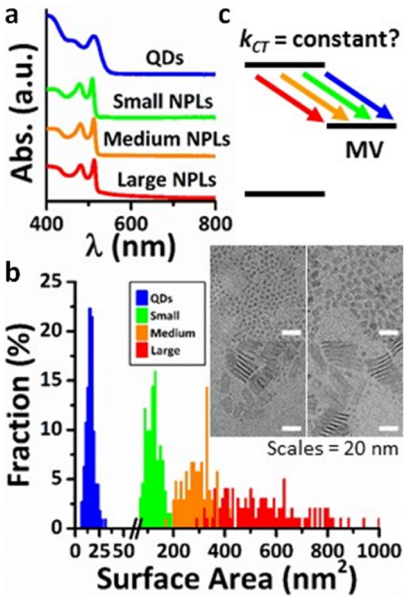

Figure 1. (a) Absorption spectra and (b) transmission electron microscopy-derived histograms relating total particle surface area of the four examined zinc blende CdSe nanoparticle samples. (c) Jablonski diagram indicating constant driving force between the nanomaterials and MV, yet CT rates shown below systematically differ.

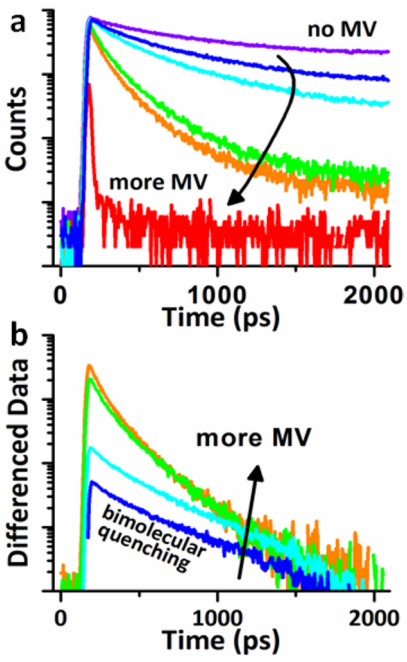

Figure 2. (a) Raw PL dynamics of large CdSe NPLs in solution upon the addition of increasing amounts of MV, here from 3.1 to 310 μM, with correspondingly faster decay dynamics. (b) Differenced data obtained by normalizing time-resolved PL traces such as in panel (a) at long times and subtracting the nanoparticle-only signal without MV. Curves are maintained in the same color in (a) and (b).

these colloidal quantum wells, photophysical studies, via comparison of time-resolved absorption, photoluminescence (PL), and terahertz transmission as well as theory relate that photogenerated electron−hole pairs remain bound as excitons,[29,30] which recombine radiatively and do not generate high-mobility free carriers as observed in some nanostructures with quantum confinement overwhelmingly in the surface normal dimension.[31−33]

To determine CT time constants that exclusively involve electron transfer from the exciton to MV, streak camera-based time-resolved photoluminescence (trPL) experiments were performed on dispersions of the four colloidal nanoparticles (spherical QDs and three sizes of CdSe NPLs, all having the same bandgap) as a function of [MV] and compared with stock dispersions of the nanoparticles. Care was taken to identify the regime of only a single MV per quenched nanoparticle as noted below. In all measurements, the optical excitation fluence was maintained well-below the multiexciton regime so as to only examine the scenario of a single photoexcited electron−hole pair per nanoparticle, and solutions were rapidly stirred to avoid charging effects. PL quenching experiments were performed using dilutions of MV salt added to chloroform dispersions of NPLs or QDs. MV rapidly adsorbs on both cadmium- and sulfur-terminated surfaces of related CdS nanoparticles, with large associated adsorption energies in excess of −3.5 eV.[8] Association can occur through direct adsorption to exposed stoichiometric surfaces and displacement of cadmium-bound carboxylates, and we expect similar adsorption processes in the case of CdSe. The implemented trPL technique has advantages over transient absorption measurements to obtain quenching rates, namely, the ability to readily distinguish several decades of PL decay with low excitation fluence and observe quenching in only a small fraction of the ensemble such that examination of the effect of just one MV per particle can be readily obtained. Further, though transient absorption offers higher time resolution than the trPL measurements used here, the data in Figure 2 indicate that such high resolution is unnecessary, particularly in the low [MV] regime.

As MV is added to the nanoparticle-containing solution, the samples exhibit increasingly rapid decay associated with electron transfer in addition to reduced PL quantum yield (see Supporting Information Figure S1). Previous transient absorption experiments unambiguously identify electron transfer as the source of exciton quenching through the concomitant appearance of induced absorption from a MV radical.[11] Quenching times of CdSe and CdS nanocrystals vary widely in the literature, from 200 fs to >10 ps, likely depending on the MV concentration and the measurement conditions.[11,22,34−37] Recent work on electron-transfer from NPLs to MV has claimed that multiexponential behavior in quenching is related to facet-dependent adsorption and transfer rates,[38] but it is also true that higher concentrations of MV adsorbates necessarily yield multiexponential, faster quenching behavior in ensembles, which we herein attempt to avoid. Since it is clear in Figure 2a that electron transfer rates increase with [MV], any useful comparison of the relative CT rates as a function of nanoparticle size or faceting requires the isolation of the quenching rate associated with a single MV adsorption.

We extract the CT time constant for each NC−MV pair in these measurements by examining low MV concentrations where MV adsorption should occur for only a small fraction of total particles in the sample (<5%). To determine the bimolecular MV quenching rate, trPL data are normalized at ∼2 ns and the contribution of particles with MV adsorption is isolated by subtracting the nanoparticle-only control signal. As MV is added in a 2:1 solution of chloroform/methanol, the trPL control sample was also examined with the addition of an equivalent volume of clean solvent, which was not observed to alter the displayed dynamics. This analysis presents similarity to extracting

DOI: 10.1021/jacs.6b06572
J. Am. Chem. Soc. 2016, 138, 11109−11112

biexcitonic Auger decay time constants[39] and is only valid under conditions in which MV-derived quenching does not contribute significantly to the trPL decay at the normalization point or dramatically alter the rates of other recombination processes. Further the differencing and normalization implemented isolates CT related to MV and removes the influence of any interparticle stacking or trapping processes that might occur in the nanoparticle-only samples.[29,40]

Figure 2b shows that at sufficiently low concentrations of MV the differenced dynamics (i.e., the MV-related quenching component) are insensitive to further dilution of [MV], consistent with Poisson statistics and indicative of domination of a 1:1 nanoparticle to MV stoichiometry for quenched nanoparticles. Conversely, where large numbers of quencher are present per nanoparticle, differenced dynamics would exhibit continuously changing decay rates with broad distributions of numbers of MV per nanoparticle. Concentration-independent decay curves (in this dilute limit) also bolster the notion of MV binding to the particle surface. The bimolecular CT decay time constant is extracted by fitting the differenced data to a single exponential in this concentration-insensitive regime. Further, because Poisson statistics of adsorption predict substantial contributions from trimolecular and higher order quenching approaching molar ratios of 1:1, accurate determination of the bimolecular rate without deconvolution of higher-order quenching necessitates that any adsorption should occur, on average, in only a small percentage of nanoparticles (<10%).

Similar experiments were performed for all nanoparticles. Specifically, three samples of four-monolayer-thick (1.4 nm) CdSe NPLs were grown with increasing lateral dimensions of 9.4 nm × 4.2 nm (termed small), 16.5 nm × 7.2 nm (medium), and 26.2 nm × 8.6 nm (large). Bimolecular CT data and fitted exponential decays, again differenced from each respective nanoparticle stock solution, appear in Figure 3a. Clearly, as the extent of the nanoparticles increases, the time for CT to a single adsorbed MV increases from ∼60 ps for the CdSe QD sample, consistent with earlier work,[22] to >300 ps for the largest NPL sample (as shown in Figure 3b).

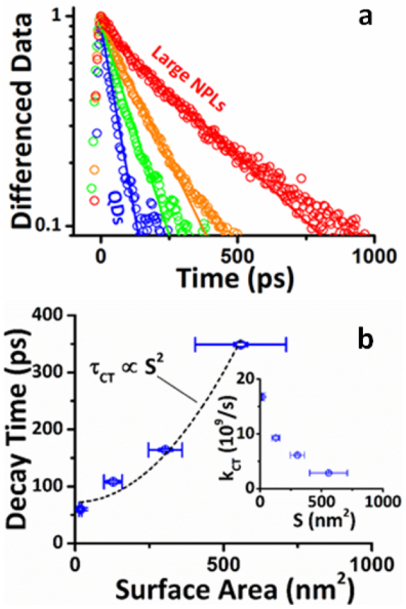

Figure 3. (a) Extracted bimolecular decay traces for the four samples. Thin lines represent exponential fits. (b) Bimolecular quenching lifetime ($1/k_{CT}$) versus per particle surface area. The dotted line relates a quadratic dependence. Inset shows the charge transfer rate plotted versus surface area. Horizontal error bars represent the standard deviation particle areas; vertical error bars represent fitting error.

The dependence of CT time constants on total particle surface area, S, exhibits two notable features. For small, near-zero surface area (derived from spherical QD-MV CT data), the CT time constant is of course finite, ∼60 ps, owing to typical features of Marcus Theory such as a given free energy change and a particular electronic coupling. Interestingly, as surface area increases, a superlinear, possibly quadratic, dependence of the quenching time becomes evident. Moreover, assuming uncorrelated quenching events at higher [MV], quantitative support for a quadratic dependence of the quenching time on S is further supported by examination of differenced data; specifically data collected at an MV concentration of 31 μM (green curve Figure 1b) can be fitted with a triexponential decay in which the decay times represent Poissonian subpopulations with $n = 1, 2, 3$ bound MV molecules. The data fitting shows substantial agreement with lifetimes following $\tau_n = \tau_{n=1}/n^2$ (see also Figure S3).

The quadratic dependence of the quenching time is a natural consequence of the coherent dynamics of the exciton center of mass.[27,41] Assuming excitons are delocalized over greater lateral extent for larger NPLs, an approximate single-determinant excitonic wave function[30] for the singlet (superscript S) has the simple form:[42]

$$\psi^S = \phi_c(z_e)\phi_v(z_h)\chi_k(\rho_e)\chi_k(\rho_h)\xi(|\rho_e - \rho_h|, z_e, z_h)$$

with $\phi_{c/v}$ the quantum-confined components along the z direction, χ the delocalized in-plane component, and ξ the envelope function. Following previous work, an NPL of width L, the real-space normalized valence and conduction wave functions can be approximately written as[43]

$$\phi_n(z) = \sqrt{2/L}\,\cos(\pi n z/L), \quad \chi_k(\rho) = e^{i\rho k}/\sqrt{L}$$

where k is the in-plane quasi-momentum. The in-plane normalization factor in the latter expression naturally leads to $\psi^S \propto 1/S$. Assuming the electron, following CT, fully localizes on the MV molecule, the Coulomb potential experienced by the holes in a thin dielectric slab has been derived by Kumagai and Takagahara[44] and does not depend on the slab area. Then, the CT-state transition rate given by the Fermi Golden Rule

$$\Gamma^{S\to CT} \propto \frac{2\pi}{\hbar}|\langle\psi^{CT}|V|\psi^S\rangle|^2$$

yields the experimentally observed quadratic dependence of the quenching time for highly coherent excitons freely moving within the NPL.

Finally, because our model relates that delocalization is significant in the 2D CdSe morphology, we examined relative optical absorption for a film of NPLs to determine whether oscillator strength changes substantively for reduced temperature, where prior time-resolved studies have suggested giant oscillator strength emergence.[27,45] As shown in Figure S7a, variation of temperature did result in some narrowing of ensemble absorption line width, but not to a degree beyond simple thermal broadening. Fitting and integration of a spectral line shape (similar results for Gaussian and Lorentzian) considering the lowest-energy transition showed no elevation of oscillator strength with reduced temperature, which suggests rather constant delocalization in the NPLs. In further support of

DOI: 10.1021/jacs.6b06572
J. Am. Chem. Soc. 2016, 138, 11109−11112

this point, the temperature-dependent energy gap also followed typical Varshni behavior as presented in Figure S7b.

In conclusion, we have shown experimentally that for a fixed free energy change, nanomaterials can exhibit a CT rate that depends significantly on the particle spatial extent. Through examinations of trPL dynamics with increasing concentration of an electron acceptor, we identified bimolecular CT time constants as noted by a regime of quencher concentration independence in the dilute limit. By comparing such times for an isoenergetic series of nanoparticles, we were able to identify a dependence of CT time on surface area that slowed nonlinearly with increasing NPL area, which we attribute to exciton motion in the structure. We believe that this type of surface area dependence can offer broad relevance to understanding optoelectronic function in chemically- and physically prepared 2D materials including desired CT behavior, as well as undesired trapping behavior. Further, this study opens a door to examinations of the interplay of coherent exciton dynamics in the presence of localized CT states in these same materials classes.

■ ASSOCIATED CONTENT

Supporting Information

The Supporting Information is available free of charge on the ACS Publications website at DOI: 10.1021/jacs.6b06572.

Additional details of syntheses and experimental data (PDF)

■ AUTHOR INFORMATION

Corresponding Author

*schaller@anl.gov or schaller@northwestern.edu

Notes

The authors declare no competing financial interest.

■ ACKNOWLEDGMENTS

This work was performed in part at the Center for Nanoscale Materials, a US Department of Energy, Office of Science, Office of Basic Energy Sciences User Facility under Contract No. DE-AC02-06CH11357.

■ REFERENCES

(1) Kovalenko, M. V.; Manna, L.; Cabot, A.; Hens, Z.; Talapin, D. V.; Kagan, C. R.; Klimov, V. I.; Rogach, A. L.; Reiss, P.; Milliron, D. J. *ACS Nano* **2015**, *9*, 1012.

(2) Kamat, P. V. *J. Phys. Chem. Lett.* **2013**, *4*, 908.

(3) Marcus, R. A. *J. Chem. Phys.* **1956**, *24*, 966.

(4) Kamat, P. V. *J. Phys. Chem. C* **2008**, *112*, 18737.

(5) Robel, I.; Kuno, M.; Kamat, P. V. *J. Am. Chem. Soc.* **2007**, *129*, 4136.

(6) Choi, J. J.; Lim, Y.-F.; Santiago-Berrios, M. E. B.; Oh, M.; Hyun, B.-R.; Sun, L.; Bartnik, A. C.; Goedhart, A.; Malliaras, G. G.; Abruña, H. D.; Wise, F. W.; Hanrath, T. *Nano Lett.* **2009**, *9*, 3749.

(7) Hyun, B.-R.; Bartnik, A. C.; Lee, J.-K.; Imoto, H.; Sun, L.; Choi, J. J.; Chujo, Y.; Hanrath, T.; Ober, C. K.; Wise, F. W. *Nano Lett.* **2010**, *10*, 318.

(8) Peterson, M. D.; Jensen, S. C.; Weinberg, D. J.; Weiss, E. A. *ACS Nano* **2014**, *8*, 2826.

(9) Zhu, H.; Yang, Y.; Wu, K.; Lian, T. *Annu. Rev. Phys. Chem.* **2016**, *67*, 259.

(10) Knowles, K. E.; Tice, D. B.; McArthur, E. A.; Solomon, G. C.; Weiss, E. A. *J. Am. Chem. Soc.* **2009**, *132*, 1041.

(11) Zhu, H.; Yang, Y.; Hyeon-Deuk, K.; Califano, M.; Song, N.; Wang, Y.; Zhang, W.; Prezhdo, O. V.; Lian, T. *Nano Lett.* **2014**, *14*, 1263.

(12) Wu, K.; Liang, G.; Shang, Q.; Ren, Y.; Kong, D.; Lian, T. *J. Am. Chem. Soc.* **2015**, *137*, 12792.

(13) Sykora, M.; Petruska, M. A.; Alstrum-Acevedo, J.; Bezel, I.; Meyer, T. J.; Klimov, V. I. *J. Am. Chem. Soc.* **2006**, *128*, 9984.

(14) Rawalekar, S.; Kaniyankandy, S.; Verma, S.; Ghosh, H. N. *J. Phys. Chem. C* **2009**, *114*, 1460.

(15) Bridewell, V. L.; Alam, R.; Karwacki, C. J.; Kamat, P. V. *Chem. Mater.* **2015**, *27*, 5064.

(16) Tarafder, K.; Surendranath, Y.; Olshansky, J. H.; Alivisatos, A. P.; Wang, L.-W. *J. Am. Chem. Soc.* **2014**, *136*, 5121.

(17) Tansakul, C.; Lilie, E.; Walter, E. D.; Rivera, F.; Wolcott, A.; Zhang, J. Z.; Millhauser, G. L.; Braslau, R. *J. Phys. Chem. C* **2010**, *114*, 7793.

(18) Hyun, B.-R.; Bartnik, A.; Sun, L.; Hanrath, T.; Wise, F. *Nano Lett.* **2011**, *11*, 2126.

(19) Zhu, H.; Song, N.; Lian, T. *J. Am. Chem. Soc.* **2010**, *132*, 15038.

(20) Morris-Cohen, A. J.; Frederick, M. T.; Cass, L. C.; Weiss, E. A. *J. Am. Chem. Soc.* **2011**, *133*, 10146.

(21) Tachiya, M. *J. Chem. Phys.* **1982**, *76*, 340.

(22) Dworak, L.; Wachtveitl, J. *Z. Phys. Chem.* **2011**, *225*, 575.

(23) Johnson, M. D.; Miller, J. R.; Green, N. S.; Closs, G. L. *J. Phys. Chem.* **1989**, *93*, 1173.

(24) Berlin, Y. A.; Ratner, M. A. *Radiat. Phys. Chem.* **2005**, *74*, 124.

(25) Bhimanapati, G. R.; Lin, Z.; Meunier, V.; Jung, Y.; Cha, J.; Das, S.; Xiao, D.; Son, Y.; Strano, M. S.; Cooper, V. R.; Liang, L.; Louie, S. G.; Ringe, E.; Zhou, W.; Kim, S. S.; Naik, R. R.; Sumpter, B. G.; Terrones, H.; Xia, F.; Wang, Y.; Zhu, J.; Akinwande, D.; Alem, N.; Schuller, J. A.; Schaak, R. E.; Terrones, M.; Robinson, J. A. *ACS Nano* **2015**, *9*, 11509.

(26) Ithurria, S.; Dubertret, B. *J. Am. Chem. Soc.* **2008**, *130*, 16504.

(27) Ithurria, S.; Tessier, M. D.; Mahler, B.; Lobo, R. P. S. M.; Dubertret, B.; Efros, A. L. *Nat. Mater.* **2011**, *10*, 936.

(28) She, C.; Fedin, I.; Dolzhnikov, D. S.; Dahlberg, P. D.; Engel, G. S.; Schaller, R. D.; Talapin, D. V. *ACS Nano* **2015**, *9*, 9475.

(29) Kunneman, L. T.; Schins, J. M.; Pedetti, S.; Heuclin, H.; Grozema, F. C.; Houtepen, A. J.; Dubertret, B.; Siebbeles, L. D. A. *Nano Lett.* **2014**, *14*, 7039.

(30) Benchamekh, R.; Gippius, N. A.; Even, J.; Nestoklon, M.; Jancu, J.-M.; Ithurria, S.; Dubertret, B. 1.; Efros, A. L.; Voisin, P. *Phys. Rev. B: Condens. Matter Mater. Phys.* **2014**, *89*, 035307.

(31) Knox, W.; Fork, R.; Downer, M.; Miller, D.; Chemla, D.; Shank, C.; Gossard, A.; Wiegmann, W. *Phys. Rev. Lett.* **1985**, *54*, 1306.

(32) Kunneman, L. T.; Zanella, M.; Manna, L.; Siebbeles, L. D. A.; Schins, J. M. *J. Phys. Chem. C* **2013**, *117*, 3146.

(33) Schmitt-Rink, S.; Chemla, D.; Miller, D. *Adv. Phys.* **1989**, *38*, 89.

(34) Dworak, L.; Matylitsky, V. V.; Breus, V. V.; Braun, M.; Basché, T.; Wachtveitl, J. *J. Phys. Chem. C* **2011**, *115*, 3949.

(35) Jiang, Z.-J.; Kelley, D. F. *J. Phys. Chem. C* **2011**, *115*, 4594.

(36) Matylitsky, V. V.; Dworak, L.; Breus, V. V.; Basché, T.; Wachtveitl, J. *J. Am. Chem. Soc.* **2009**, *131*, 2424.

(37) Zhu, H.; Song, N.; Rodríguez-Córdoba, W.; Lian, T. *J. Am. Chem. Soc.* **2012**, *134*, 4250.

(38) Okuhata, T.; Tamai, N. *J. Phys. Chem. C* **2016**, *120*, 17052.

(39) Klimov, V. I.; Mikhailovsky, A.; McBranch, D.; Leatherdale, C.; Bawendi, M. G. *Science* **2000**, *287*, 1011.

(40) Rabouw, F. T.; van der Bok, J. C.; Spinicelli, P.; Mahler, B.; Nasilowski, M.; Pedetti, S.; Dubertret, B.; Vanmaekelbergh, D. *Nano Lett.* **2016**, *16*, 2047.

(41) Cassette, E.; Pensack, R. D.; Mahler, B.; Scholes, G. D. *Nat. Commun.* **2015**, *6*, 6086.

(42) Berkelbach, T. C.; Hybertsen, M. S.; Reichman, D. R. *Phys. Rev. B: Condens. Matter Mater. Phys.* **2013**, *88*, 045318.

(43) Jena, D.; Konar, A. *Phys. Rev. Lett.* **2007**, *98*, 136805.

(44) Kumagai, M.; Takagahara, T. *Phys. Rev. B: Condens. Matter Mater. Phys.* **1989**, *40*, 12359.

(45) Naeem, A.; Masia, F.; Christodoulou, S.; Moreels, I.; Borri, P.; Langbein, W. *Phys. Rev. B: Condens. Matter Mater. Phys.* **2015**, *91*, 121302.

DOI: 10.1021/jacs.6b06572
J. Am. Chem. Soc. 2016, 138, 11109−11112